We are IntechOpen, the world's leading publisher of Open Access books
Built by scientists, for scientists

6,500
Open access books available

176,000
International authors and editors

190M
Downloads

154
Countries delivered to

Our authors are among the
TOP 1%
most cited scientists

12.2%
Contributors from top 500 universities

WEB OF SCIENCE™

Selection of our books indexed in the Book Citation Index
in Web of Science™ Core Collection (BKCI)

Interested in publishing with us?
Contact book.department@intechopen.com

Numbers displayed above are based on latest data collected.
For more information visit www.intechopen.com

Chapter

Fabrication of Variable Morphologies on Argon Sputtered PMMA Surfaces

Divya Gupta, Rimpi Kumari, Amena Salim, Rahul Singhal and Sanjeev Aggarwal

Abstract

Ion beam induced patterning and fabrication of various topographies over polymeric surfaces has drawn strong interest due to latent applications in photonics, magnetic devices, optical devices and photovoltaics etc. In this work, we report the controlled surface structuring and evolution of different morphologies in Poly(methyl methacrylate) polymer using Ar^{+} ion beam fabrication technique. Morphological and structural analysis has been performed by ex situ Atomic Force Microscopy (AFM) and X-ray Diffraction. The effect of oblique incidences on argon sputtered films was evaluated by various surface topography and texture parameters, such as Fast Fourier Transforms, surface roughness, skewness, kurtosis. AFM study demonstrates fabrication of transient morphologies over argon sputtered surfaces. One dimensional (1D) cross section scans of surface profiles are determined and morphological features are investigated. The results showed halo peaks in the XRD patterns, which indicate the amorphous nature of this type of polymer. The formation of these surface structures is attributed to the different degree of sputtering yield at different off-normal incidences and preferential sputtering of hydrogen in comparison to carbon in ion sputtered surfaces.

Keywords: PMMA, argon ion irradiation, atomic force microscopy, X-ray diffraction, sputtering

1. Introduction

Surface structuring and patterning of polymers by ion irradiation is a technique that involves exposing a polymer surface to ion beam to selectively modify its structural and chemical properties. This technique allows the creation of complex patterns with high resolution and precision, making it highly valuable in a range of fields, such as microelectronics, sensors, and biomedical applications [1–10].

During the process of ion irradiation, the incident ions penetrate the polymer surface and cause a series of physical and chemical changes, such as chain scission, cross-linking, and the formation of new chemical groups. These changes can be controlled by adjusting the beam parameters such as ion energy, ion dose, and angle of

IntechOpen

incidence, allowing the creation of a range of patterns with different geometries and varying depths.

One of the key advantages of ion irradiation induced structuring and patterning is its ability to create highly uniform patterns over a large area, making it ideal for large-scale manufacturing. Furthermore, this technique can be applied to a range of polymers, including those that are difficult to pattern using conventional lithography techniques [1–11].

Ion beam induced patterning and structuring in materials is a rapidly evolving field with a wide range of applications, including micro- and nanofabrication, surface modification, and materials engineering. Reports are available in the existing literature describing the use of this versatile technique for creation of diverse morphologies over different classes of materials [12–23].

Vazquez et al. [12] have given an up-dated account of the progress reached when surface composition plays a relevant role, with a main focus on ion beam irradiation surface patterning with simultaneous co-deposition of foreign atoms. Further, they have reviewed the advances in ion beam irradiation of compound surfaces as well as ion beam irradiation systems where the ion employed is not a noble gas species. Additionally, they have explained the main theoretical models aimed at describing these nanopattern formation processes. Lastly, they have addressed two main special features of the patterns induced by this ion beam irradiation technique, namely the enhanced pattern ordering and the possibility to produce both morphological and chemical patterns.

Cuerno et al. [13] have presented a perspective investigation on the main developments that have led to the current understanding of nanoscale pattern formation at surfaces by ion-beam irradiation, from the points of view of experiments, applications, and theory, and offer an outlook on future steps that may eventually facilitate full harnessing of such a versatile avenue to materials nanostructuring.

They have started with a brief survey on the key issues which have been dealt with up to the recent past with respect to both experiments and applications and theoretical aspects of IBS surface nanopatterning. Then, they have assessed the current status of open problems which we consider important, again providing perspectives on these from the points of view of experiments and applications and also from the theoretical and computational viewpoints. For definiteness, they have restricted the discussion to the patterns formed by low energy ($E_{ion} \lesssim 10$ keV), broad ion beams, albeit with occasional mention of results at higher energies.

Valbusa et al. [14] have studied that the surface etching by ion sputtering can be used to pattern surfaces. Recent studies using the high-spatial-resolution capability of the scanning tunneling microscope revealed in fact that ion bombardment produces repetitive structures at nanometer scale, creating peculiar surface morphologies ranging from self-affine patterns to fingerprint-like and even regular structures, for instance waves (ripples), chequerboards or pyramids. The phenomenon is related to the interplay between ion erosion and diffusion of adatoms (vacancies), which induces surface re-organization. Their paper reviews the use of sputter etching to modify 'in situ' surfaces and thin films, producing substrates with well-defined vertical roughness, lateral periodicity and controlled step size and orientation.

Li et al. [15] have studied the recent Applications of Ion Beam Techniques on Nanomaterial Surface Modification and hence design of Nanostructures and Energy Harvesting. According to them, ion beam techniques have extensively been applied for modulating the performance of various nanomaterials. In addition, ion beam techniques have also been used to fabricate nanomaterials, including 2D materials,

nanoparticles, and nanowires. In addition, ion beam techniques exhibit high controllability and repeatability. The recent progress in ion beam techniques for nanomaterial surface modification is systematically summarized and existing challenges and potential solutions are presented.

Gupta et al. [16] have studied the controlled surface modification and nanodots structures over Si(111) surfaces produced by oblique angle sputter deposition of 80 keV Ar + beam. Temporal parameters such as self-assemble, tunability of size and density of fabricated nano-dots exhibited distinct fluence dependence. Crystalline to amorphous (c/a) phase transition for sputter deposited Si(111) surfaces has been observed. RBS/C reveals the non-linear response of damage distribution with argon ion fluence. The underlying self-organization mechanism relied on ion beam sputtering induced erosion and re-deposition of Si atoms thereby leading to mass transport inside the created amorphous layers.

They have [17] also studied the controlled surface structuring of amorphous silicon carbide (a-SiC) thin films as grown on silicon substrates Si(111) by Radio Frequency (RF) sputtering and irradiation of obliquely incident 80 keV Ar^+ ion beam has been investigated. Sub-wavelength ripple patterns with wave-vector parallel to the ion beam projection are found to evolve on argon sputtered surfaces. Studies reveal that the temporal parameters such as ripple wavelength and amplitude, ordering and homogeneity of these patterns vary non-linearly with argon ion fluence. The formation of such surface structures is attributed to the preferential sputtering of silicon in comparison to carbon.

Goyal et al. [19, 20] have studied the temporal variations in nano-scale surface morphology generated on Polypropylene (PP) substrates by 40 keV argon ion sputtering. Formation of ripple patterns and its transition to dot morphology has been realized. Switching of smoothing mechanism from ballistic drift to ion enhanced surface diffusion is the most probable cause for such morphological transition.

Kumari et al. [21] have investigated the patterning of HDPE surfaces by oblique argon ion irradiation. Formation of ripple patterns and its transition to sideways bars & valleys has been observed. Further, transition from parallel to perpendicular mode patterns has been seen. Curvature dependent sputtering and role of various smoothing processes describes the observed surface patterning.

Overall, these studies demonstrate the diverse and exciting potential applications of ion beam-induced patterning and structuring in materials, and highlight the ongoing development of new techniques and mechanisms to control and manipulate these structures.

Hence, motivated by the universality of this IBS technique and pivotal applications of patterned polymeric surfaces, here, we have made an attempt in present endeavor to explore the controlled patterning of poly(methyl methacrylate) PMMA surface by obliquely incident Ar^+ beam erosion with optimized ion beam parameters.

2. Materials and methods

The PMMA studied, was procured from Goodfellow Ltd. (UK). The samples used were flat rectangular wafers of 1 mm thickness.

These specimens were then sputtered with 30 keV Ar^+ ions at an oblique incidence of 0°, 15°, 30°, 40°, 50°, 75° with respect to sample surface. The ion beam sputtering experiments were carried out at room temperature using 200 kV Ion Accelerator [24], which is available in Ion Beam Centre, KUK. The beam current density of 0.5 $\mu A/cm^2$

was used to sputter the samples. The argon fluence was kept constant at 2×10^{16} ions/cm^2.

The morphological evolution of these sputtered surfaces has been examined by Atomic Force Microscopy (AFM) utilizing Bruker HR Multimode-8 instrument. The surfaces were scanned in scan-asyst tapping mode with Antimony(n) doped Si cantilever tip. Different types of scans were obtained at random places on the sample surface. The scanned areas (10×10 μm^2) were sampled at 256 equidistant points at low scan rate of 1 Hz. The scanned images were examined using NanoScope 1.8 software. The observed surface features were evaluated using section analysis and Fast Fourier Transformations (FFTs) of corresponding AFM images.

Structural analysis has been performed employing Bruker AXS D8 Advance X-ray diffractometer using Cu Kα X-ray (λ = 1.5406 Å).

3. Results and discussion

3.1 Morphological analysis

Figure 1a–g presents the two dimensional (2D) topography image of the un-irradiated and 30 keV Ar^+ sputtered PMMA surface at various incident angles of 75° to 15° keeping ion fluence fixed at 2×10^{16} Ar^+ cm^{-2}. The scanned size for these images is 10×10 μm^2. The consequent FFT (Fast Fourier Transform) of micrographs has also been illustrated in 2D AFM images. The qualitative analysis of these AFM images in terms of temporal parameters (obtained through section analysis of respective AFM images) have been calculated using Nanoscope 1.8 software and are presented in **Table 1**.

It is clear from **Figure 1a** that the surface is smooth in nature. Corresponding Fast Fourier Transform (FFT) reveals the smoothness of the un-treated PMMA polymer surface.

Prominent changes in surface morphology can be easily trailed from the comparison of AFM micrograph of **Figure 1a** with **Figure 1b–g**.

After argon ion irradiation at an off-normal incidence of 90°, the rough surface transform into pits with irregular hills. The corresponding FFT image depicts the increase in ordering and homogeneity of the evolved surface features.

With a subsequent decrease in angle of incidence to 75°, the hill morphology becomes prominent with simultaneous occurrence of pits (**Figure 1c**). The enhanced ordering of the evolved hill morphology can be easily deduced from the respective FFT image as shown in inset.

Fascinatingly, with further decrease in angle of incidence to 50°, irregular wavy features in place of pits on the surface can be easily seen in **Figure 1d**. Also, change in the preferred orientation of the surface features can be inferred from the inset image.

As the sputtering proceeds and angle of incidence decreases to 40°, the ripple morphology becomes prominent and pit morphology disappears. These wavy features have orientation parallel to the ion beam direction. The increase in ordering of ripple morphology can be easily observed from the inset images.

With prolonged decrease in angle of incidence to 30°, similar behavior has been observed. Here, also early stages of ripple formation can be clearly seen from the AFM image as shown in **Figure 1f**. This ripple morphology has wave-vectorial orientation parallel to the ion beam direction. Enhanced ordering among the evolved surface structures can be easily deduced from the respective FFT image.

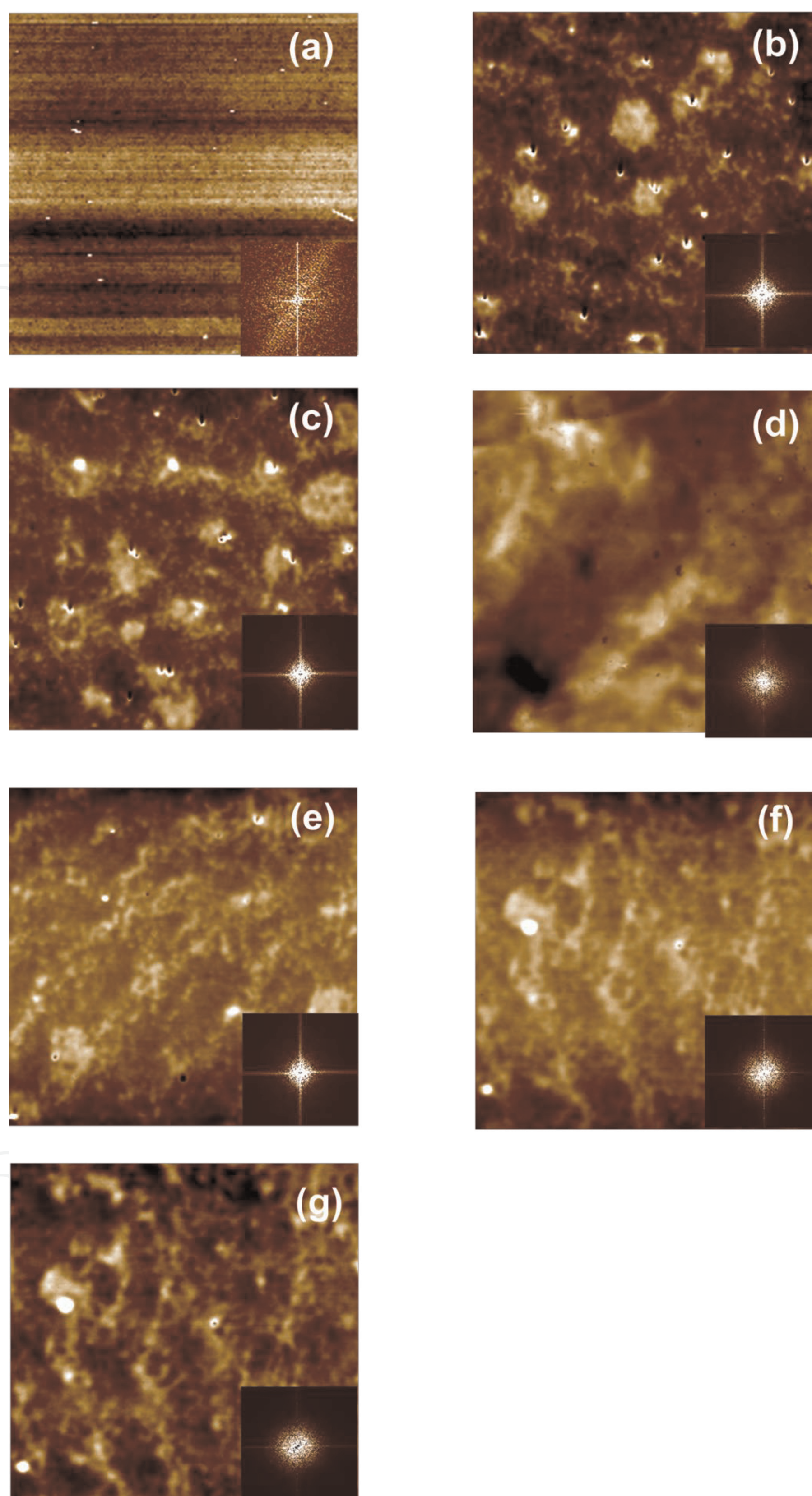

Figure 1.
2D AFM micrographs of for (a) untreated PMMA and irradiated with 30 keV argon ions to a fluence of 2×10^{16} ions/cm^2 at oblique incidences of (b) 90°, (c) 75°, (d) 60°, (e) 50°, (f) 40°, (g) 15° with respect to sample surface.

Similar behavior of surface morphology can be observed at lowest oblique incidence of 15°. Presence of wavy patterns over the sample surface can be easily seen from the AFM image as shown in **Figure 1g**. corresponding FFT image reveals the ordering of the surface features.

Figure 2 presents the one-dimensional line scans of AFM micrographs for PMMA irradiated with 30 keV argon ions to a fluence of 2×10^{16} ions/cm^2 at oblique incidences of (a) 90°, (b) 75°, (c) 60°, (d) 50°, (e) 40°, (f) 15° with respect to sample surface.

It is clear from **Figure 2** that for normal incidence of argon ions, the surface morphology is majorly dominated by pits. Thereafter, gradual switching to wavelike morphology can be easily inferred from the line scans.

3.2 Qualitative description

Surface RMS roughness is a common parameter used to quantify the surface roughness of a sample in Atomic Force Microscopy (AFM) images. It is a statistical measure that describes the average deviation of the height of the sample surface from its mean value over a given area [1–7]. Hence, keeping this in mind, we have calculated the RMS roughness by Nanoscope 1.8 software. The surface roughness for these sputtered surfaces is summarized in **Table 1**.

Moreover, skewness is a statistical measure that describes the degree of asymmetry in a distribution of data. In general, a positive skewness value indicates that the height distribution is skewed to the right, meaning that there are more high points on the surface than low points. A negative skewness value indicates that the height distribution is skewed to the left, meaning that there are more low points on the surface than high points. A skewness value of zero indicates that the height distribution is

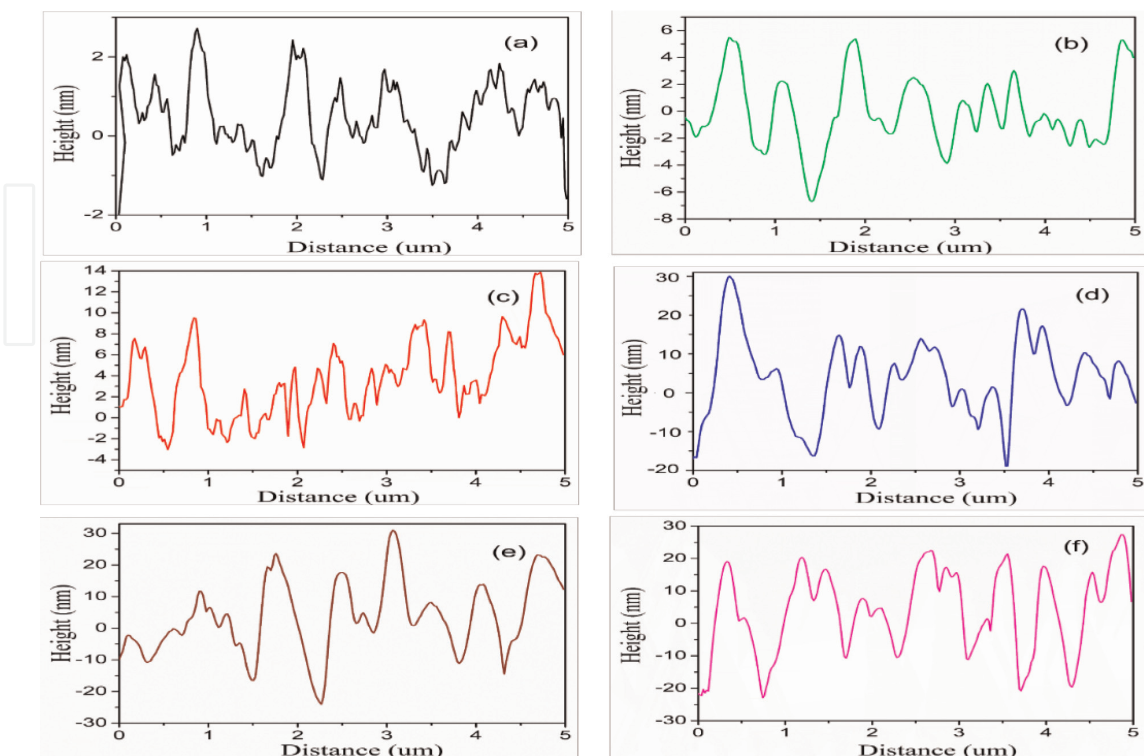

Figure 2.
Time evolution of the line scans with the ion incident angle.

S. No.	PMMA sputtered with oblique incidence of	RMS Roughness (nm)	Skewness	Kurtosis
1.	Untreated	03 ± 0.20	0.11	3.04
2.	90°	10.5 ± 1.20	0.23	3.25
3.	75°	13.1 ± 1.40	0.25	3.18
4.	60°	24.32 ± 3.20	0.26	3.08
5.	50°	15.8 ± 2.30	0.42	3.36
6.	40°	12.61 ± 1.80	0.44	3.34
7.	15°	11 ± 1.60	0.48	3.38

Table 1.
Values of RMS roughness, skewness and kurtosis as a function of angle of incidence.

symmetric, meaning that there are equal numbers of high and low points on the surface [1–5].

Kurtosis is a statistical measure that characterizes the shape, or "peakedness," of a distribution. In the context of Atomic Force Microscopy (AFM) images, kurtosis can be used to analyze the surface roughness and topography of the sample being imaged [2–6].

Specifically, the kurtosis of an AFM image quantifies the degree to which the height distribution of the image deviates from a normal or Gaussian distribution. A high kurtosis value indicates that the height distribution has a sharp peak and heavy tails, while a low kurtosis value indicates a flatter distribution with less pronounced tails [1–7].

By analyzing skewness, kurtosis along with RMS roughness, a more complete picture of the surface morphology has been obtained and these parameters as a function of angle of incidence are listed in **Table 1.**

Table 1 clearly reveals that the surface roughness varies non-linearly with the angle of incidence of argon ions. The surface roughness for untreated PMMA surface is found to be 03 ± 0.20 nm which again confirms the smoothness over the sample surface. Interestingly, with sputtering at normal incidence, the surface roughness increases abruptly. This in turn reveals the roughening of the initial smooth surface. RMS roughness increases continuously with decrease in ion incidence to 60°. This clearly point towards the roughening of the PMMA sample surface. Thereafter, the surface roughness decreases leading to smoothening of the surface.

Moreover, positive value of skewness reveals the presence of hill morphology or ripple morphology above the sample surface. Furthermore, value of nearly 3 for kurtosis indicates the peakedness of the observed morphology over the sample surface.

3.3 Structural analysis

The X-ray diffraction patterns of untreated and 30 keV argon ion irradiated PMMA specimens with a fluence of 2×10^{16} ions/cm^2 at oblique incidences of 90°, 75°, 60°, 50°, 40°, 15° with respect to sample surface are shown in **Figure 3**.

The diffraction pattern of un-treated PMMA specimen shows a broad and intense peak centered at 14.24° with one lower intensity signal centered at 29.70°. The presence of later signal is attributed to the diffuse scattering of amorphous PMMA specimen.

The shape of the first main signal indicates the ordered packing of the polymer chains. The intensity and shape of the second signal are attributed to the effect

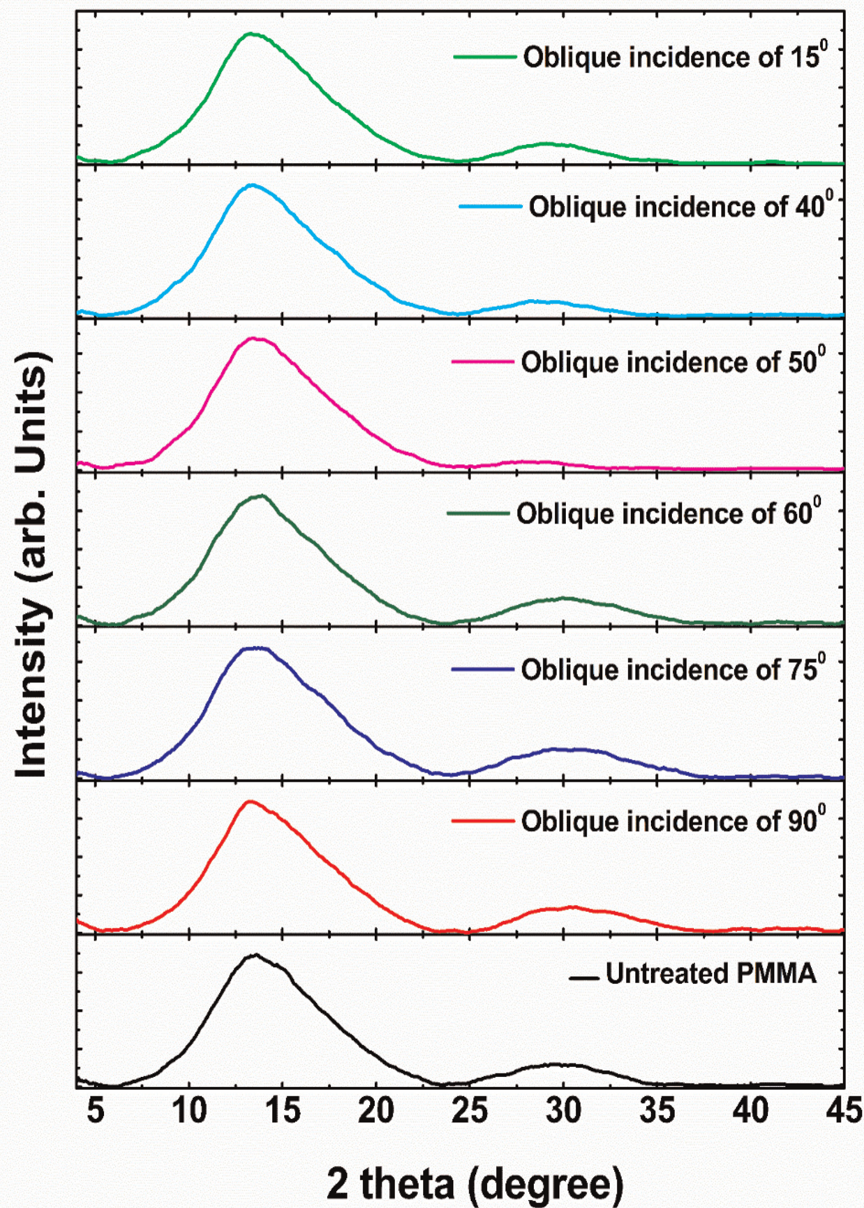

Figure 3.
X-ray diffraction pattern for untreated PMMA and irradiated with 30 keV argon ions to a fluence of 2×10^{16} ions/cm^2 at oblique incidences of 90°, 75°, 60°, 50°, 40°, 15° with respect to sample surface.

occurring inside the main chains in the polymeric matrix. The observed broad humps in the XRD spectrum indicate the presence of crystallites of very low dimensions. Further, the absence of prominent peaks in this XRD analysis indicates the amorphous nature of the PMMA polymer [25, 26].

The XRD pattern for PMMA samples sputtered with 30 keV argon ions shows no appreciable change in the peak position and Intensity.

For complete insights into the structural behavior, the crystallite size (a) has been determined using Scherrer's formula [25].

$$a = \frac{0.94\lambda}{\beta cos\theta} \tag{1}$$

Where β is the full width at half maxima (FWHM), λ is the wavelength of the x-ray beam and θ is the diffraction angle.

Values of crystallite size have been summarized in **Table 2**.

Table 2 reveals that the crystallite size varies non-linearly with angle of incidence of argon ions. Crystallite size is always smaller pointing towards the amorphous nature of the surface region.

3.4 TRIM simulations

TRIM (Transport and Range of Ions in Matter), simulation code, is widely used to study the effect of energetic ion bombardment on the different properties of materials, such as surface erosion, sputtering, and implantation [27].

In the present work, we have performed these TRIM simulations to calculate the projected range of incident argon ions at different ion incidences with respect to surface normal and sputtering yield of different components of target matrix.

Figure 4 presents the variation in energy transferred to recoiling atoms for different ion incidences of argon.

It is clear from **Figure 4** that with decrease in angle of incidence, the energy transferred to recoiling atoms increases. This clearly point towards more surface disordering with decrease in angle of incidence.

It can be inferred from **Table 3** that for normal incidence, the incoming argon ions penetrate deep into the polymeric matrix. The projected range is maximum for normal incidence of argon ions. As the angle of incidence of incoming ions decreases, the projected range decreases. For lowest oblique incidence, projected range is found to be the lowest. Interestingly, the sputtering yield increases with decrease in angle of incidence of the argon ions. Sputtering yield is found to be maximum for lowest oblique incidence under present case.

The observed morphological and structural behavior can be explained in terms of sputtering yield, energy to recoils and projected range variations with angle of incidence. Basically, two phenomena occur upon energetic ion irradiation of polymeric matrix: one is the scissioning of polymeric chains which results in bond breaking and shortening of chains predominantly occur as a result of nuclear energy loss process and the other is cross-linking and conjugation mainly due to electronic energy loss process [1]. Both these processes correspond to the roughening and smoothing of polymeric surface which consequences in spontaneous pattern formation triggered by surface instability.

Angle of incidence	2θ (°)	FWHM (°)	a (nm)
Untreated	14.24	7.13	1.17 ± 0.01
90°	14.25	7.07	1.18 ± 0.02
75°	14.24	7.38	1.13 ± 0.01
60°	14.23	7.30	1.15 ± 0.02
50°	14.14	7.20	1.16 ± 0.01
40°	14.13	7.16	1.17 ± 0.02
15°	14.13	7.10	1.18 ± 0.03

Table 2.
Values of Bragg angle, FWHM and crystallite size as a function of angle of incidence.

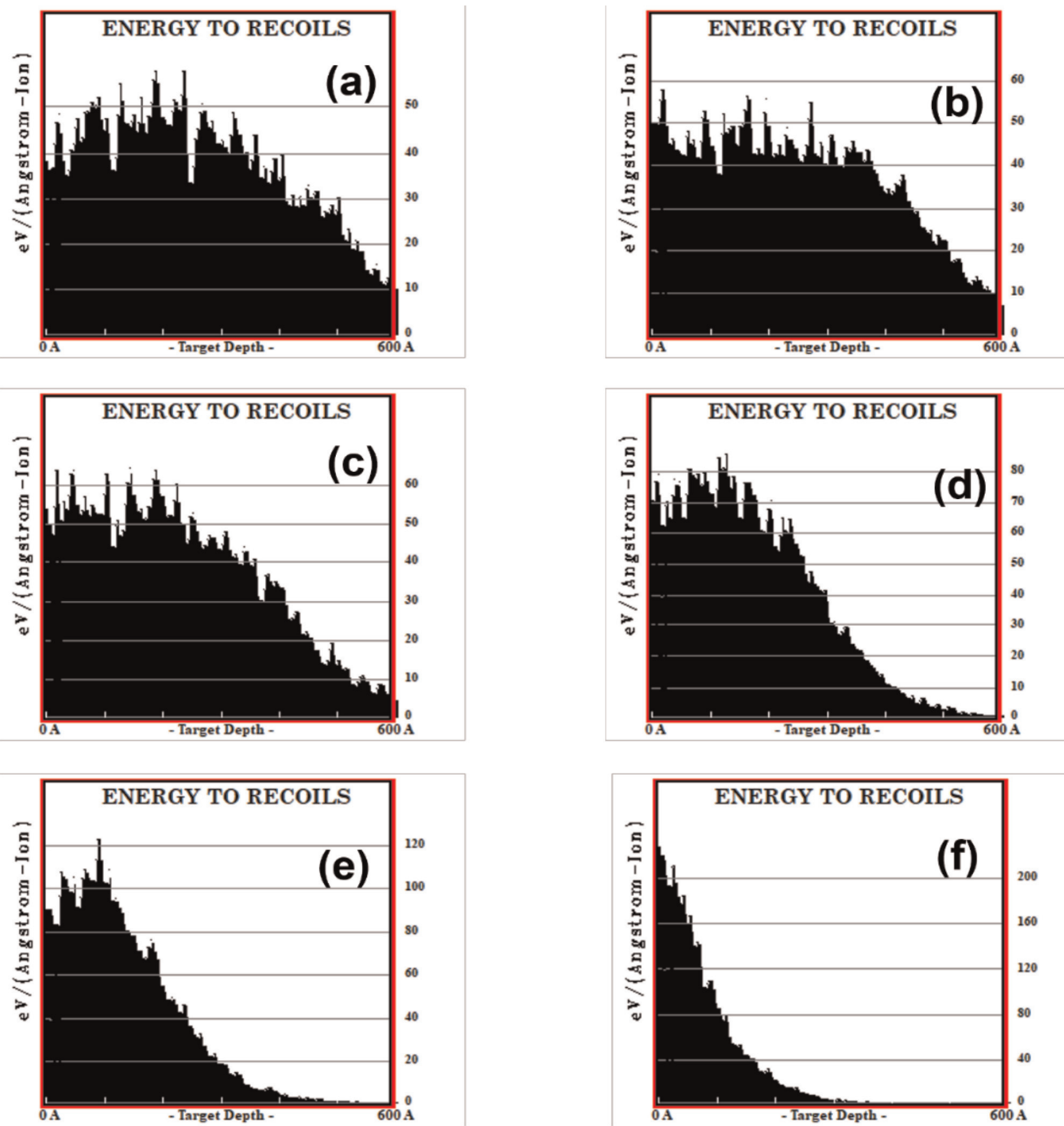

Figure 4.
Energy transferred to recoiling atoms for different argon ion incidences.

PMMA sputtered at ion incidence of	Projected range (nm)	Sputtering yield of hydrogen (atom/ion)	Sputtering yield of carbon (atom/ion)	Sputtering yield of oxygen (atom/ion)
90°	51.4 ± 14.3	1.06	0.22	0.24
75°	49.6 ± 14.2	1.18	0.26	0.27
60°	44.4 ± 13.6	1.80	0.46	0.45
50°	39.3 ± 13.1	2.55	0.69	0.64
40°	33.0 ± 12.4	3.86	1.11	0.96
15°	16.2 ± 08.8	14.34	4.58	3.74

Table 3.
Values of projected range, sputtering yield of hydrogen, carbon and oxygen as a function of angle of incidence.

For normally incident argon ions, the projected range is more and energy transferred to recoiling atoms is less. This results in more structural damage of the polymeric matrix leading to the formation of pit morphology. Interestingly, lower

sputtering yields of carbon, hydrogen and oxygen further adds to the formation of pits inside the surface due to more disordering induced inside the surface.

With decrease in angle of incidence to 75°, the projected range decreases and energy to recoils increases. This further produces pit morphology but with less pronounced effect. The increase in sputtering yield of carbon, hydrogen and oxygen causes more surface disordering leading to the formation of pit morphology but majorly in the surface region.

With further decrease in oblique incidence, the projected range deceases gradually and energy transferred to recoiling atoms increases significantly. The increase in sputtering yield of carbon, hydrogen and oxygen has been observed. All these factors result in more surface disordering leading to wave like patterns in place of pit morphology.

At lowest oblique incidence, projected range decreases while energy transferred to recoils increases. Further, sputtering yield increases abruptly leading to only alterations in surface region. Hence, prominent wavy patterns are observed at this stage under present experimental conditions.

4. Conclusions

In summary, we report the controlled surface structuring and evolution of different morphologies in Poly(methyl methacrylate) (PMMA) polymer using Ar^+ ion beam fabrication technique. Morphological and structural analysis has been performed by ex situ Atomic Force Microscopy (AFM) and X-ray Diffraction. The effect of oblique incidences on argon sputtered films was evaluated by various surface topography and texture parameters, such as Fast Fourier Transforms, surface roughness, skewness, kurtosis. AFM study demonstrates fabrication of transient morphologies over argon sputtered surfaces. One dimensional (1D) cross section scans of surface profiles are determined and morphological features are investigated. The results showed halo peaks in the XRD patterns, which indicate the amorphous nature of this type of polymer. The formation of these surface structures is attributed to the different degree of sputtering yield at different off-normal incidences and preferential sputtering of hydrogen in comparison to carbon in ion sputtered surfaces.

Acknowledgements

This research was primarily supported by the Department of Science and Technology (DST), New Delhi for funding major research project for utilizing 200 kV Ion Accelerator and related characterization facilities. Authors are thankful to the Ministry of Human Resource and Development (MHRD) for RUSA 2.0 grants for Centre for Advanced Material Research (CAMR) to Kurukshetra University. Authors are indebted to Dr. Dinakar Kanjilal, Raja Ramana Fellow, and Dr. Sundeep Chopra, Inter University Accelerator Centre (IUAC), New Delhi for fruitful discussions. We are thankful to Dr. P. C. Kalsi (Retd.), Scientist-H, Radiochemistry Division, BARC, Mumbai for useful comments and constructive insights.

IntechOpen

Author details

Divya Gupta[1*], Rimpi Kumari[1], Amena Salim[2], Rahul Singhal[2] and Sanjeev Aggarwal[1]

1 Ion Beam Centre, Department of Physics, Kurukshetra University, Kurukshetra, India

2 Department of Physics, Malviya National Institute of Technology (MNIT), Jaipur, India

*Address all correspondence to: divyagupta2017@kuk.ac.in

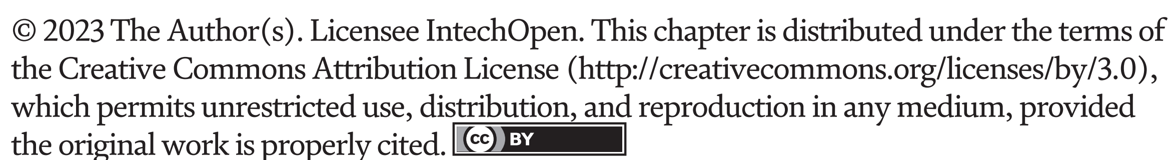

IntechOpen

© 2023 The Author(s). Licensee IntechOpen. This chapter is distributed under the terms of the Creative Commons Attribution License (http://creativecommons.org/licenses/by/3.0), which permits unrestricted use, distribution, and reproduction in any medium, provided the original work is properly cited.

References

[1] Zhao YP, Wang GC, Lu TM. Characterization of Amorphous and Crystalline Rough Surfaces: Principles and Applications. San Diego: Academic Press; 2001

[2] Bennett JM, Mattsson L. Introduction to Surface Roughness and Scattering. Washington, DC: Optical Society of America; 1989

[3] Eklund EA, Snyder EJ, Williams RS. Correlation from randomness: Quantitative analysis of ion-etched graphite surfaces using the scanning tunnelling microscope. Surface Science. 1993;**285**:157. DOI: 10.1016/0039-6028(93)90427-L

[4] Eklund EA, Snyder EJ, Williams RS. Submicron-scale surface roughening induced by ion bombardment. Physical Review Letters. 1991;**67**:1759

[5] Jacobs TDB, Junge T, Pastewka L. Quantitative characterization of surface topography using spectral analysis. Surface Topography: Metrology and Properties. 2017;**5**:13001

[6] Gupta D, Chawla M, Singhal R, Aggarwal S. Nanoscale structural defects in oblique Ar^{+} sputtered Si (111) surfaces. Scientific Reports. 2019;**9**:15531

[7] Wei Q, Lian J, Zhu S, Li W, Sun K, Wang L. Ordered nanocrystals on argon ion sputtered polymer films. Chemical Physics Letters. 2008;**452**:124-128. DOI: 10.1016/j.cplett.2007.12.053

[8] Slepicka P, Nedela O, Sajdl P, Kolska Z, Svorcík V. Polyethylene naphthalate as an excellent candidate for ripple nanopatterning. Applied Surface Science. 2013;**285**:885-892. DOI: 10.1016/j.apsusc.2013.09.007

[9] Facsko S, Dekorsy T, Koerdt C, Trappe C, Kurz H, Vogt A, et al. Formation of ordered nanoscale semiconductor dots by ion sputtering. Science. 1999;**285**:1551-1553

[10] Bradley RM, Harper JME. Theory of ripple topography induced by ion bombardment. Journal of Vacuum Science and Technology A. 1988;**6**:2390-2395

[11] Moon MW, Han JH, Vaziri A, Her EK, Oh KH, Lee KR, et al. Nanoscale ripples on polymers created by focussed ion beam. Nanotechnology. 2009;**20**:115301-115308. DOI: 10.1088/0957-4484/20/11/115301

[12] Vázquez L, Cubero AR, Lorenz K, Palomares FJ, Cuerno R. Journal of Physics: Condensed Matter. 2022;**34**:333002. DOI: 10.1088/1361-648X/ac75a1

[13] Cuerno R, Kim JS. A perspective on nanoscale pattern formation at surfaces by ion beam irradiation. Journal of Applied Physics. 2020;**128**:180902

[14] Valbusa U, Boragno C, Mongeot FB. Nanostructuring surfaces by ion sputtering. Journal of Physics: Condensed Matter. 2002;**14**:8153-8175

[15] Li WQ, Zhan XY, Song XY, Si SY, Chen R, Liu J, et al. A review of recent applications of ion beam techniques on nanomaterial surface modification: Design of nanostructures and energy harvesting. Small. 2019;**31**:901820. DOI: 10.1002/smll.201901820

[16] Gupta D, Kumari R, Umapathy GR, Singhal R, Ojha S, Sahoo PK, et al. Self-assembled nano-dots structures on Si (111) surfaces by oblique angle sputter-deposition. Nanotechnology. 2019;**30**:

385301-385312. DOI: 10.1088/1361-6528/ab273a

[17] Gupta D, Umapathy GR, Singhal R, Ojha S, Aggarwal S. Ripple patterns over oblique Ar+ sputtered SiC/Si(111) surfaces: Role of preferential sputtering. Materials Letters. 2019;**307**(4):131011. DOI: 10.1016/j.matlet.2021.131011

[18] Buatier de Mongeot F, Valbusa U. Applications of metal surfaces nanostructured by ion beam sputtering. Journal of Physics: Condensed Matter. 2009;**21**:224022. DOI: 10.1088/0953-8984/21/22/224022

[19] Goyal M, Aggarwal S, Sharma A, Ojha S. Surface structuring in polypropylene using Ar^+ beam sputtering: Pattern transition from ripples to dot nanostructures. Applied Surface Science. 2018;**439**:380-385. DOI: 10.1016/j.apsusc.2018.01.002

[20] Goyal M, Gupta D, Aggarwal S, Sharma A. Self-organized nanopatterning of polycarbonate surfaces by argon ion sputtering. Journal of Physics: Condensed Matter. 2018;**30**:284002-284009. DOI: 10.1088/1361-648X/aac966

[21] Kumari R, Gupta D, Singhal R, Sharma A, Aggarwal S. Surface patterning of high density polyethylene by oblique argon ion irradiation. Journal of Applied Physics. 2019;**126**:155303-155310. DOI: 10.1063/1.5116889

[22] Bradley RM. Theory of nanoscale ripple topographies produced by ion bombardment near the threshold for pattern formation. Physical Review E. 2020;**102**:012807. DOI: 10.1103/PhysRevE.102.01280

[23] Sigmund P. Theory of sputtering. I. Sputtering yield of amorphous and polycrystalline targets. Physics Review. 1969;**184**:383. DOI: 10.1103/PhysRev.184.383

[24] Gupta D, Aggarwal S, Sharma A, Kumar S, Chopra S. 200 kV ion accelerator Facility at Kurukshetra University, India. Materials Letters. 2022;**308**:131294

[25] Lee JH, Won J, Jeong H-C, Kim DH, Lee DW, Han J-M, et al. Physicochemical analysis of ion beam-induced surface modifications on polyethylene glycol films for liquid crystal alignment. Liquid Crystals. 2019;**46**(12):1799-1807. DOI: 10.1080/02678292.2019.1606351

[26] Gnaser H, Reuscher B, Zeuner A. Propagation of nanoscale ripples on ion-irradiated surfaces. Nuclear Instrument Methods B. 2012;**285**:142. DOI: 10.1016/j.nimb.2012.05.028

[27] Zeigler JF, Ziegler MD, Biersack JP. SRIM 2008.04 software package. Available online: http://www.srim.org